Experimental and Theoretical Study of Water Retention Effects on Elastic Properties of Opalinus Shale

Alexey Yurikov*
Curtin University
26 Dick Perry Avenue,
Kensington, WA, 6151
alexey.yurikov@postgrad.curtin.edu.au

Maxim Lebedev
Curtin University
26 Dick Perry Avenue,
Kensington, WA, 6151
m.lebedev@curtin.edu.au

Marina Pervukhina
CSIRO Energy
26 Dick Perry Avenue,
Kensington, WA, 6151
Marina.Pervukhina@csiro.au

Boris Gurevich
Curtin University, CSIRO
26 Dick Perry Avenue,
Kensington, WA, 6151
b.gurevich@curtin.edu.au

**presenting author asterisked*

SUMMARY

Understanding of shales elastic properties behaviour with saturation changes is important for geological storage of nuclear waste, CO_2 sequestration as well as for development of conventional and unconventional shale oil and gas reservoirs. Existing data describing effects of saturation on elastic properties of shales are sparse and contradictory. To improve understanding of the effects of changing water content on elastic properties in shales, we conduct an experimental study on Opalinus shale samples. We measure vertical and horizontal ultrasonic P- and S-wave velocities of the same set of samples with controlled water content. The measured velocities are used to calculate components of elastic stiffness tensor in the shale at different saturations assuming its vertical transverse isotropy. Obtained results show increasing C_{11} and decreasing C_{33} with drying of the samples. Moreover, we observe 80% and 60% increase of shear moduli C_{44} and C_{66}, respectively, with reduction of the water content from 5.5% weight in the preserved state to 0.3%. Conventional rock physics models are not designed to explain the observed dynamics. Here we perform a theoretical investigation of the influence on the shale moduli of following factors: (1) mechanical softening of the rock with the decrease of water saturation; (2) shrinkage of clay leading to reduction of porosity; (3) chemical hardening of clay particles; and (4) enhancing stiffness of contacts due to removing of water between clay particles.

Key words: rock physics, shale, desorption, elastic properties.

INTRODUCTION

The interest in geomechanical behaviour of shales rises nowadays as this type of rock is often involved in many engineering applications such as safe geological storage of nuclear waste, CO_2 sequestration, and both conventional and unconventional hydrocarbon extraction. Exploitation of shales as seals or reservoirs could induce changing of saturation in these rocks. Recent studies show that variations of water content influence both microstructures and elastic properties of shales. For instance, Montes *et al*. (2004) reported Environmental Scanning Electron Microscope (ESEM) observations showing complex cracking and particle aggregation and desegregation in argillite with changing water content. Vales *et al*. (2004) observed a significant shrinkage of Tournemire shale samples containing 40% clay with desiccation and reported a decrease of ultrasonic compressional wave velocity V_P in the direction perpendicular to the bedding plane with the decrease of water content, while the shrinkage along the bedding was small and V_P in this direction was constant. Ghorbani *et al*. (2009) reported increasing compressional and shear wave velocities (V_P and V_S respectively) measured along and perpendicular to the bedding for clay-rocks with drying. Other studies (e.g., Romero *et al*., 2011; Salager *et al*., 2013; Ferrari *et al*., 2014) showed decrease of porosity in compacted clayey soils with desiccation and rehydration.

Despite intensive efforts during last decade, the effect of changing water content on elastic properties of shales is not fully understood. Recently, a number of attempts to tie elastic properties variations with microstructural changes in shales occurring with drying/rehydration were made. Vales *et al*. (2004) suggested to separate the water existing in shale into two types: 1) "easy-to-remove" water located in macropores and 2) water absorbed in the thin clay layers or tiny isolated pores. Later Romero *et al*. (2011), using mercury intrusion porosimetry (MIP), showed two types of porosity presenting in clays: 1) microporosity with characteristic size of pores ~10 μm constituting inter-aggregate pores, and 2) nanoporosity ~10 nm constituting intra-aggregate pores. Saturation of Romero's clayey samples leaded to swelling of nanopores and closing of micropores as demonstrated by MIP data and ESEM images. Ghorbani *et al*. (2009) also stated that changing saturation influences textural structure of clay matrix resulting in consolidation and hardening of clay particles with drying, which agrees with shrinkage of shale samples observed by Vales *et al*. (2004). However, Vales *et al*. (2004) and Ghorbani *et al*. (2009) reported the opposite dependencies of V_P measured across the bedding plane on saturation, which implies that the variations of elastic properties of shales with changing water content are driven by several competing phenomena. Moreover, Ghorbani *et al*. (2009) observed that shear moduli of shales strongly depend on water content while most conventional rock physics models (e.g., Gassmann, 1951) imply that shear modulus is independent on fluid saturation of the rock.

The lack of data and comprehensive understanding of shale elastic moduli behaviour with varying water content impelled this study. In this work we measure ultrasonic V_P and V_S of Opalinus shale samples with different water saturation that is achieved by desiccating the samples under controlled relative humidity. Then we derive the elastic tensor component dependencies on water

content in the samples. Using the experimental data, we investigate the influence of the following factors on the shale elastic properties: (1) mechanical softening of the rock with substitution of saturating water with gas; (2) shrinkage of clay leading to reduction of porosity; (3) chemical hardening of clay particles; and (4) enhancing stiffness of contacts due to removing a water lubricant between clay particles.

EXPERIMENTAL APPROACH

Samples

The aim of this study is to investigate influence of varying water content on elastic properties of shales. In order to measure elastic properties we selected two disc-shaped (~15 mm long, 38 mm in diameter) samples cut vertically and horizontally from the Opalinus shale without use of cooling/lubricating water to preserve the initial water content. The Opalinus shale is well-known rock used for many experimental studies (e.g., Soe *et al*., 2009; Monfared *et al*., 2014; Minardi *et al*., 2016). It contains >80% clay matrix with porosity 10-20%, which is mostly constituted by pores smaller than 1 μm (Houben, 2013).

The mineralogy of the samples used for this work is determined by X-ray diffraction (XRD) analysis as 16% kaolinite, 42% illite-smectite, 10% illite/mica, 4% chlorite, 14% quartz, 9% calcite, 1% pyrite, 1% siderite, 1% albite/anorthite, 1% anatase, <1% dolomite/ankerite, <1% rutile. To obtain the grain density and water saturation, a small sample of the Opalinus shale is crashed into powder and is dried in a vacuum chamber at 105 degrees Celsius to evaporate all removable water. Then, the grain density of the shale is determined with gas pycnometer as 2.66 g/cm^3. The water content in the preserved samples is determined by the change of mass of the powder before and after drying as 5.5% mass fraction and saturation is estimated as 95%.

Desiccation and ultrasonic measurements

We change water content in tested samples by maintaining them in enclosed glass chambers (desiccators) with presence of different solutes controlling relative humidity (RH) (e.g., Greenspan, 1977) at ambient temperature. Starting with preserved state of the samples, we follow a drying path consequently placing the samples in desiccators with 52%, 31%, and 13% RH, which gives four saturation states. During desiccation we monitor the samples mass change keeping them in the same atmosphere until the mass is stabilized, which usually takes up to three weeks. At the end of each desiccation stage (including the starting preserved state), we determine elastic properties of the shale by velocity measurements of ultrasonic P- and S-waves propagating along the axis of the disc samples. The experimental technique is described in Yurikov *et al*. (2016). When the measurements are conducted on the horizontally cut sample, the S-wave is polarized in the bedding plane. Therefore, we measure $V_P(0°)$, $V_P(90°)$, $V_{SV}(0°)$, and $V_{SH}(90°)$ and, assuming vertical transverse isotropy (VTI) of the Opalinus shale samples, calculate components of the stiffness tensor (Mavko *et al*., 2009):

$$C_{11} = \rho V_P^2(90°);\ C_{33} = \rho V_P^2(0°);\ C_{44} = \rho V_{SV}^2(0°);\ C_{66} = \rho V_{SH}^2(90°). \quad (1)$$

Here, the bulk density of the samples ρ is experimentally determined on the sister samples that undergone the same drying path. We weight the duplicates immersed in oil and derive bulk density of the samples at each saturation state:

$$\rho = \rho_{oil}\left[1 - \frac{W_{im}}{mg}\right]^{-1}, \quad (2)$$

where ρ_{oil} is the density of oil, g is the gravitational acceleration, m is the mass of the sample, and W_{im} is the weight of the same sample immersed in oil.

Continuous mass monitoring allows determining water mass fraction in the samples. It can be done for each desiccation stage by iterative procedure knowing the mass (m) and water mass fraction (ω) in the sample at the previous stage:

$$\omega = 1 - \frac{m_{previous}}{m}(1 - \omega_{previous}). \quad (3)$$

The determined water content, grain density (ρ_{gr}), and bulk density (ρ) of the samples allows to estimate evolution of porosity with drying:

$$\varphi = 1 - \frac{\rho}{\rho_{gr}}(1 - \omega). \quad (4)$$

EXPERIMENTAL DATA

Table 1 shows the results of the Opalinus samples characterization after each stage of the desiccation experiment. The consecutive drying of the samples leads to the decrease of water content down to 0.3%. Bulk density also reduces with drying as a result of two competing, albeit related, factors: water desorption and shrinkage of the samples. The estimations also show porosity reduction with desiccation, which agrees with results of Salager *et al*. (2013) and the others. The shown experimental errors result from indirect measurements of presented parameters and limited number of samples (only two).

The results of the Opalinus shale elastic properties measurements are reported in Figure 1. The shear moduli C_{44} and C_{66} show, respectively, the gradual 80% and 60% increases with drying from the initial preserved state to 0.3% of water mass fraction. The C_{11} and C_{33} behaviour differs from that demonstrated by shear moduli. The C_{11} remains constant at 31 GPa till the last desiccation stage when it shows the 34% increase up to 42 GPa. The C_{33} exhibits the opposite trend showing the drastic decrease from 18 to 11 GPa after the first desiccation stage and remains almost constant afterwards. Such behavior of elastic moduli differs from that previously reported by Vales *et al*. (2004) and Ghorbani *et al*. (2009).

Table 1. Characterization of Opalinus shale at the end of each stage of the desiccation experiment.

	Preserved	52% RH	31% RH	13% RH
ω, %	5.5 ± 0.4	2.5 ± 1.1	1.3 ± 0.7	0.3 ± 0.8
ρ, g/cm^3	2.44 ± 0.03	2.38 ± 0.01	2.37 ± 0.01	2.36 ± 0.01
φ, %	13.6 ± 2.5	13.1 ± 1.9	12.2 ± 1.7	11.8 ± 1.7

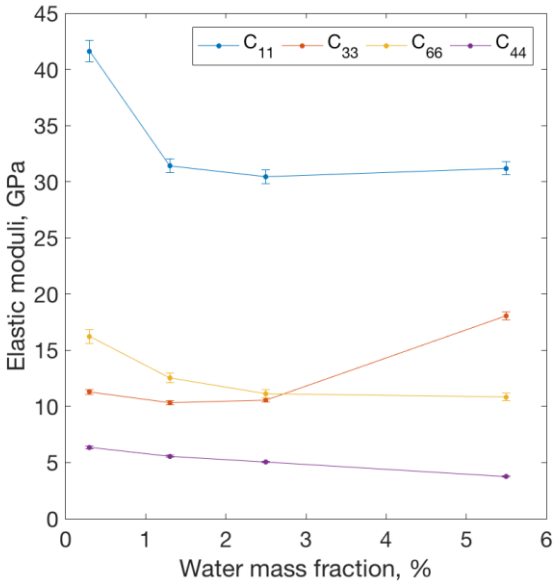

Figure 1. Elastic moduli dependency on water content in the Opalinus shale.

DISCUSSION

The diversity of existing experimental data implies that effects of saturation/desiccation on elastic properties of shales is a complex phenomenon driven by multiple competing factors. The first factor is reduction of water saturation in pores with desiccation. This effect is well known in the poroelasticity and is usually modelled by a fluid substitution model (Gassmann, 1951) or in anisotropic cases by Brown and Korringa (1975). The second factor is porosity reduction as a consequence of desorption induced deformations of the shale leading to the increase of elastic moduli. The third factor is a hardening of clay particles comprising the shale with desiccation (e.g., Ebrahimi *et al*., 2012; Carrier *et al*., 2014). The fourth factor is the stiffening of contacts between clay particles as the result of desorption of lubricating water (e.g., Osipov *et al*., 2004). We investigate the sensitivity of elastic properties of the Opalinus shale to these factors using the existing experimental data.

Fluid substitution and reduction of porosity

We analyse the influence of the water content and porosity reduction on the elastic properties of the shale as joint factors. We use the experimental data reported in Table 1 and describe the elastic properties dependency on these factors with the Differential Effective Medium (DEM) theory (Nishizawa, 1982). The DEM model allows predicting elastic properties of a composite media comprised of a background material, or matrix, and embedded inclusions with known elastic properties and concentrations. We use the model assuming that the pores in the shale are represented as spheroid shape inclusions with the aspect ratio α. We also assume that the measured porosity is comprised of the pores with the same aspect ratio, and all the water is located inside these pores. Therefore, the saturation of the samples is estimated as

$$s = \frac{\rho_{gr}}{\rho_w}\frac{1/\varphi - 1}{1/\omega - 1}, \tag{5}$$

where ρ_w is the density of water assumed to be equal to 1.03 g/cm^3. We use the following workflow to predict the dependency of elastic properties on water content and porosity reduction with drying.

1) The elastic properties of the preserved shale are taken as a reference point. We inverse the DEM algorithm to derive the elastic properties of the background matrix, C_{ij}^{matrix} by removing the inclusions with concentration equal to porosity at the initial preserved state. The bulk modulus of the inclusions representing pores saturated with water-air mix is calculated using Reuss average:

$$K_{inc}^{-1} = sK_w^{-1} + (1 - s)K_{air}^{-1}, \tag{6}$$

where $K_w = 2.2$ GPa and $K_{air} = 0.1$ GPa are the bulk moduli of water and air. The saturation here is calculated using Eq. 5. The shear modulus of the fluid-filled inclusions is zero.

2) We tie the experimentally measured porosity and water mass fraction to each other through the suction S, which is proportional to the relative humidity:

$$S = -\frac{\rho_w RT}{M_w}\ln(\mathrm{RH}), \tag{7}$$

where R is the ideal gas constant, T is the temperature, and M_w is the molar mass of water. We plot the void ratio $e = [1/\varphi - 1]^{-1}$ and the water mass fraction ω against suction (Figure 2) and approximate e and ω with exponential and linear trends respectively as shown in Figure 2. This allows to interpolate the experimental data along the drying path.

3) We perform the forward DEM modelling of the shale elastic properties evolution with drying using the matrix stiffness tensor C_{ij}^{matrix} determined at the step 1. The interpolation of the experimental data at the step 2 allows estimating of the porosity corresponding to each water mass fraction value, and thus calculating concentration of the inclusions and their elastic properties (Eq. 5 and Eq. 6).

The described model has two parameters: a) the aspect ratio of pores α, and b) the anisotropy parameter δ (Thomsen, 1986), which is used to calculate the C_{13} (Mavko *et al*., 2009), the only not measured component of the stiffness tensor of the VTI Opalinus shale samples. The anisotropy parameter δ is subjected to physical constraints reported, for instance, by Spikes (2014). According to these constraints δ must be less then 0.36 for the preserved Opalinus shale, which is used as the initial state for the modelling. We run the modelling for a set of aspect ratios from 1.0 down to 0.1 with $\delta = 0.35$. Also, in order to estimate the sensitivity of the model to the used parameter δ we run the model with $\alpha = 0.1$ setting $\delta = 0.20$ and $\delta = 0.05$.

The elastic properties dependencies on the water content in the shale predicted by the model are shown in Figure 3 color-coded by the aspect ratio used. The δ values used for the modelling with $\alpha = 0.1$ are shown by labels next to the respective curves at the figure. The anisotropy parameter δ has no effect on the shear moduli dependency on the water content, but influences the C_{11} and C_{33}. However, the model is more sensitive to the aspect ratio variation.

The fluid substitution and reduction of porosity considered in the model have opposite effects on the C_{11} and C_{33}: the replacing water by gas leads to softening, and the pores shrinkage leads to hardening of the shale. This explains the concave shape of the prediction curves shown in Figure 3. The model allows fitting the experimental C_{33} data using the parameters α and δ, however, it is unable to explain the drastic increase of the C_{11} in the driest state. Similarly, the model does not fit the increases of the experimental shear moduli C_{44} and C_{66} with desiccation. In this case the fluid substitution has no effect on the shear moduli as the shear modulus of fluid-filled inclusions remains zero with reduction of water content. Thus, the only factor that effects the C_{44} and C_{66} is the reduction of porosity. However, as shown in Figure 3, the experimentally measured reduction of porosity from 13.6% to 11.8% leads to only 9% increase of the C_{44} and 3% increase of the C_{66} in the case of $\alpha = 0.1$. Therefore, in order to explain the experimentally observed hardening of the shale with drying, other factors should be considered.

Hardening of individual clay particles and enhancing contacts

Recently it has been shown that water adsorption significantly affects elastic properties of individual clay particles (e.g., Ebrahimi *et al*., 2012; Carrier *et al*., 2014). For example, Ebrahimi *et al*. (2012) used molecular dynamics simulations (MDS) to calculate the full elastic tensor of Wyoming Na-montmorillonite, a member of the smectite group, over the range of hydration conditions. They reported dependencies of the components of the VTI stiffness tensor on the basal layer spacing, *d*, the total thickness of a clay platelet with an adjacent water layer. The data reported in a range from *d* = 9.3 Å, the thickness of a Na-montmorillonite platelet, to *d* = 20 Å (Figure 4). It is shown that reduction of the basal layer spacing, i.e. reduction of water content, results in increase of the stiffness tensor components of the smectite particles. The values of the moduli, especially of the in-plane moduli C_{11} and C_{66}, are much higher than that obtained experimentally for the Opalinus shale samples. However, smectite particles are only one of building blocks comprising the shale. Firstly, the particles are oriented at different angles forming porous clay aggregates (e.g., Romero *et al*., 2011). Secondly, the water film lubricates contacts between the particles reducing the stiffness of clay aggregates (Osipov *et al.*, 2004).

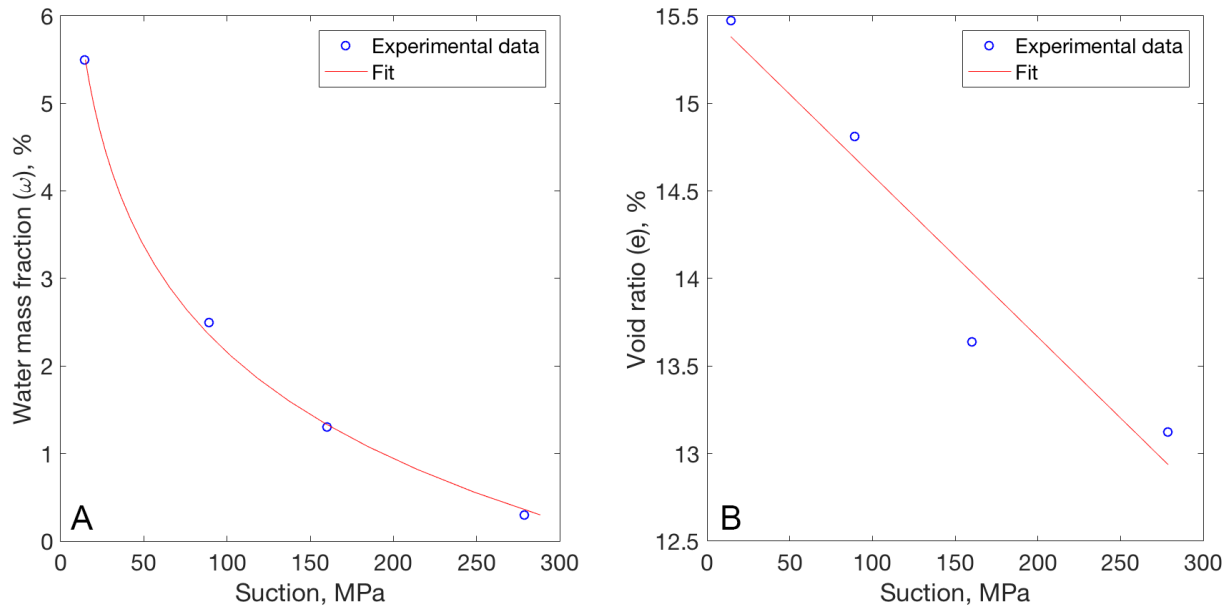

Figure 2. The experimental data versus suction. A) Water mass fraction fitted with the exponential trend. B) Void ratio fitted with the linear trend.

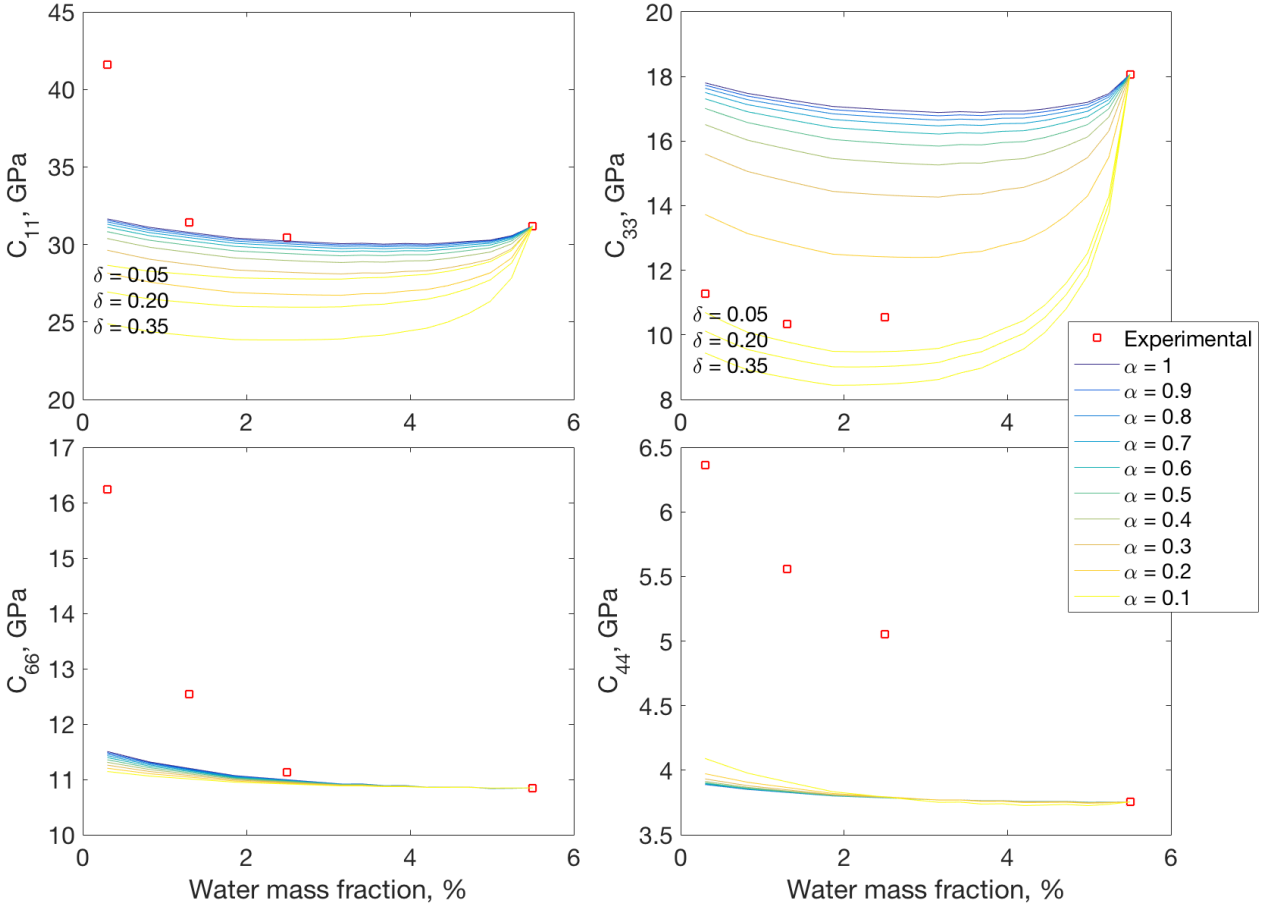

Figure 3. The dependency of elastic properties of the Opalinus shale on water content predicted by the DEM model accounting fluid substitution and porosity reduction. Aspect ratio α is color-coded. Experimental data are show with red square markers. The δ values used for the modelling with $\alpha = 0.1$ are shown by labels next to the respective curves.

In order to estimate the effect of water content dependent elastic properties of an individual smectite particle on the stiffness of the shale, we perform the calculations of elastic properties of polycrystalline clay comprised of such particles with different orientations (Shermergor, 1977). We consider two cases: 1) random orientation of the particles resulting in isotropic properties of the polycrystal, and 2) axisymmetric orientation defined by the orientation distribution function (ODF) resulting in VTI polycrystalline clay. Here, due to VTI symmetry, the ODF is a function of only the rotation angle of the normal vector of a smectite particle, θ. The MDS data shown in Figure 4 with blue markers also represents the polycrystal comprised of perfectly aligned smectite particles. This defines one of the bounds for the elastic moduli of the polycrystalline clay. The second bound is defined by the elastic properties of the polycrystal comprised of randomly distributed smectite particles (green markers). Any axisymmetric distribution of the particles would result in polycrystal elastic moduli lodged between these two bounds, as shown, for example, by the calculations with the ODF from Figure 4 (red markers).

The derived values of the polycrystalline clay elastic moduli are still much higher than that experimentally obtained for the Opalinus shale samples. However, the precise relation of the hydration state of the shale in the experiment to the basal layer spacing in clay particles is unknown and can be higher than 20 Å. To estimate the elastic properties of the clay comprised of particles with higher basal layer spacing, we fit the data calculated for axisymmetric orientation of clay particles with exponential trends and extrapolate them up to $d = 40$ Å (Figure 4). The extrapolated elastic moduli are comparable with the experimental data and can be used to describe water retention effects on elastic properties of the Opalinus shale.

The similar approach can be used to describe the enhancing stiffness of contacts between clay particles. The water layer between two clay platelets of large thickness (corresponding to high basal layer spacing values) can be considered not as a part of an individual clay particle, but as a contact between two different particles. The thickness of this contact is determined by hydration state of the clay, thus this approximation would simulate stiffness increase of clay aggregates with drying.

Building a comprehensive model

To describe the observed experimental dependencies of elastic properties on water content in shales, a comprehensive model comprising all the discussed driving factors is needed. In order to build this model, the following challenges should be addressed: 1) establishing the relation between the hydration state of the shale and the basal layer spacing of individual clay particles; 2)

establishing the relation between the hydration state of the shale and thickness of water layer at the contacts between clay particles; 3) determining the fractions of total porosity comprised by intra-aggregate nanopores and inter-aggregate micropores along with saturation of porosity of both types. While the building of a comprehensive model is interesting, it would imply thorough experimental study of pore space structure with changing water content in clays and shales, which is out of scope of this study and not available at the literature.

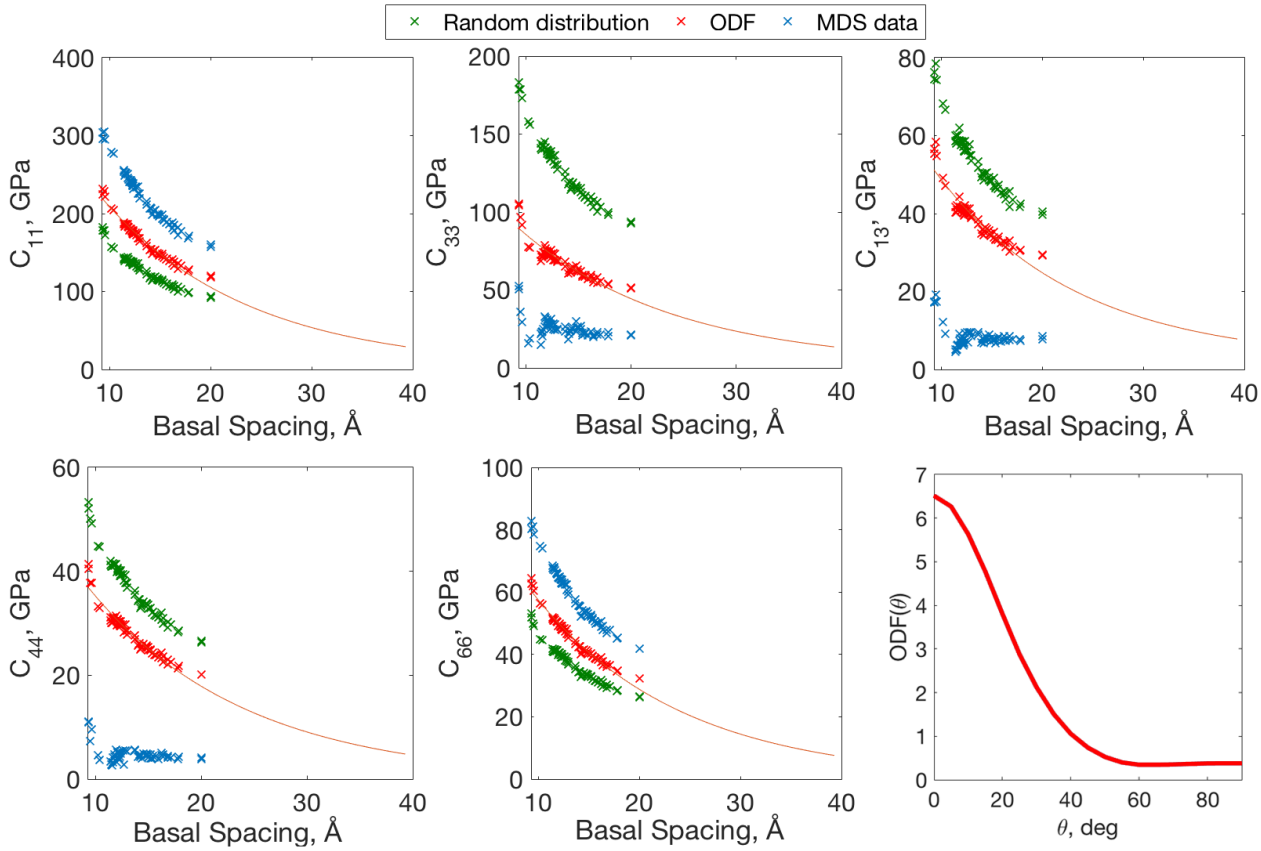

Figure 4. Elastic coefficients as a function of basal layer spacing and ODF of particles. Blue: the results of MDS modelling of VTI elastic stiffness tensor components dependencies on hydration state of an individual smectite particle, courtesy of Ebrahimi *et al.* (2012). Red: the VTI moduli of polycrystalline clay comprised of smectite particles at different hydration states with orientation defined by the ODF shown in the right bottom corner of the figure. Green: the VTI moduli of polycrystalline clay comprised of randomly distributed smectite particles at different hydration states. Thin red lines represent extrapolated exponential fits of the data calculated using ODF.

CONCLUSIONS

Water saturation effects on elastic properties and microstructure of the Opalinus shale has been experimentally studied. The water content, total porosity, and stiffness tensor components dependencies on the experienced relative humidity have been determined for the Opalinus shale samples. The results show that desiccation of the shale leads to the reduction of porosity and changes of the elastic moduli. The shear moduli C_{44} and C_{66} show continuous increase with drying up to the values ~1.5 times higher than at the initial preserved state. The C_{11} does not change much until the last desiccation stage when 34% increase is observed. The C_{33} shows the opposite trend decreasing after the first desiccation stage by 40%. The observed elastic moduli dependencies on water content in shale differ from that previously reported by Vales *et al.* (2004) and Ghorbani *et al.* (2009). This implies that elastic properties of shales are influenced by several competing factors occurring during desiccation.

In this study the following factors have been considered: (1) reduction of water saturation in pores with desiccation; (2) porosity reduction as a consequence of desorption induced deformation of the shale; (3) hardening of clay particles comprising the shale with desiccation; (4) stiffening of contacts between clay particles as the result of desorption of lubricating water. The influence of these factors on the elastic properties of the shale has been investigated. Using the differential effective medium modeling, we have shown that the (1) saturation and (2) porosity variations with drying have different effect on shear and compressional moduli of the shale. The shear moduli are not affected by fluid substitution and slightly increase due to reduction of pore space, while the compressional moduli experience combined effect of both factors. Though, this model does not explain the significant hardening of shear moduli and increase of the C_{11} at the low water content, which can be explained by (3) the hardening of individual clay particles and (4) the enhancing of contacts stiffness with drying. The influence of the last two factors on elastic properties of the shale has been studied using the results of molecular dynamics simulations (Ebrahimi *et al.*, 2012). It has been shown that clay particles exhibit increase of the elastic moduli with desorption of water stored between clay platelets. We have demonstrated that extrapolation of the numerical

simulation data on higher water content gives reasonable values of elastic moduli similar to that observed experimentally in the Opalinus shale. This data can also be used to describe the enhancing stiffness of contacts between clay particles.

ACKNOWLEDGMENTS

The authors thank Dr. Lionel Esteban for the help with the samples characterization. The authors acknowledge Dr. Roland Pellenq and Dr. Davoud Ebrahimi for sharing the data of molecular dynamic simulations used in this work. This work was partially funded by Curtin Reservoir Geophysical Consortium (CRGC). Alexey Yurikov was supported by Curtin Strategic International Postgraduate Research Scholarship and Australian Government Research Training Program Scholarship.

REFERENCES

Brown, R., and Korringa, J., 1975, On the dependence of the elastic properties of a porous rock on the compressibility of the pore fluid: Geophysics, 40, 608-616.

Carrier B., Vandamme, M. Pellenq, R. J.-M., and Van Damme, H., 2014, Elastic Properties of Swelling Clay Particles at Finite Temperature upon Hydration: The Journal of Physical Chemistry, 118, 8933-8943.

Ebrahimi, D., Pellenq, R.J.-M. and Whittle, A.J., 2012, Nanoscale Elastic Properties of Montmorillonite upon Water Adsorption: Langmuir, 28, 16855-16863.

Ferrari, A., Favero, V., Marschall, P., Laloui, L., 2014, Experimental analysis of the water retention behaviour of shales: International Journal of Rock Mechanics & Mining Sciences, 72, 61-70.

Gassmann, F., 1951, Über die Elastizität Poröser Medien. Vierteljahrsschrift der Naturforschenden Gesellschaft in Zürich: 96, 1–23.

Ghorbani, A., Zamora, M. and Cosenza, P., 2009, Effects of Desiccation on the Elastic Wave Velocities of Clay-rocks: International Journal of Rock Mechanics & Mining Sciences, 46, 1267-1272.

Greenspan, L., 1977, Humidity fixed points of binary saturated aqueous solutions: Journal of Research of the National Bureau of Standards, Section A: Physics and Chemistry, 81, 89–96.

Houben, M. E., 2013, In situ characterization of the microstructure and porosity of Opalinus Clay (Mont Terri Rock Laboratory, Switzerland): M.Sc Thesis, RWTH-Aachen University.

Mavko, G., Mukerji, T., and Dvorkin, J., 2009, The Rock Physics Handbook, 2nd edition: Cambridge University Press.

Minardi, A., Crisci, E., Ferrari, A., and Laloui, L., 2016, Anisotropic volumetric behaviour of Opalinus clay shale upon suction variation: Géotechnique Letters, 6, 144–148.

Monfared, M., Sulem, J., Delage, P., Mohajerani, M., 2014, Temperature and Damage Impact on the Permeability of Opalinus Clay: Rock Mechanics and Rock Engineering, 47, 101-110.

Montes, H.G., Duplay, J., Martinez, L., Escoffier, S. and Rousset, D., 2004, Structural Modifications of Callovo-Oxfordian Argillite Under Hydration/Dehydration Conditions: Applied Clay Science, 25, 187-194.

Nishizawa, O., 1982, Seismic velocity anisotropy in a medium containing oriented cracks - transversely isotropic case: Journal of Physics of the Earth, 30, 331-347.

Osipov, V., Sokolov, V., Eremeev, V., 2004, Clay Seals of Oil and Gas Deposits: A.A. Balkema Publishers.

Romero, E., Della Vecchia, G. and Jommi, C., 2011, An Insight Into the Water Retention Properties of Compacted Clayey Soils: Géotechnique, 61(4), 313-328.

Salager, S., Nuth, M., Ferrari, A. and Laloui, L., 2013, Investigation Into Water Retention Behaviour of Deformable Soils: Canadian Geotechnical Journal, 50, 200-208.

Shermergor, T. D., 1977, The Elasticity Theory of Microheterogeneous Media: Izd Nauka, Moscow (in Russian).

Soe, A. K. K., Osada, M., Takahashi, M., Sasaki, T., 2009, Characterization of drying-induced deformation behaviour of Opalinus Clay and tuff in no-stress regime: Environmental Geology, 58, 1215-1225.

Spikes, K. T., 2014, Error estimates of elastic components in stress-dependent VTI media: Journal of Applied Geophysics, 108, 110-123.

Thomsen, L., 1986, Weak elastic anisotropy: Geophysics, 51, 1954-1966.

Vales, F., Nguyen Minh, D., Gharbi, H. and Rejeb, A., 2004, Experimental Study of the Influence of the Degree of Saturation on Physical and Mechanical Properties in Tournemire Shale (France): Applied Clay Science, 26, 197-207.

Yurikov, A., Lebedev, M. and Pervukhina, M., 2016, Ultrasonic Measurements on Thin Samples: Experiment and Numerical Modeling: Meeting, SEG, Dallas, Technical Program Expanded Abstracts, 3338-3342.